AUSTENIT VOL. 15 NO.1, APRIL 2023 ISSN : 2085-1286 E-ISSN : 2622-7649

OPTIMIZED CONTROL OF THE PHYSICAL BATTERY SYSTEM

Pham Van De[1]*)

[1]Department of Technology, Dong Nai Technology University, Bien Hoa, Viet Nam;
*Corresponding: phamvande@dntu.edu.vn

ARTICLE INFORMATION

Revised
09/03/2023

Accepted
28/04/2023

Online Publication
05/05/2023

doi:
http://doi.org/10.5281/zenodo.7882161

ABSTRACT

Today, a significant issue for many nations worldwide is a shortage of energy. Renewable energy sources, particularly solar energy, are being investigated as additional energy sources to address the aforementioned issue. The high investment cost and poor performance of solar energy, however, provide the biggest challenge. This study only addresses the power optimization problem. It is suggested that the method used to determine the solar system's maximum power point modify incremental conductance. Adapted Incremental Conductance algorithm based on Incremental Conductance conventional techniques. The Modified Incremental Conductance method, however, has several exceptional advantages since it has a voltage change (V) that is not constant but fluctuates in an ideal manner to achieve the maximum power point as soon as possible. The voltage V is greater away from the peak power point while it is zero at the peak power point. Modified incremental conductivity algorithm to find peak power point faster than traditional algorithms. With maximum power point change reducing ambient power loss at the highest powers point. This helps to optimize voltage difference value.

***Keywords**: Photovoltaic (PV), A resizing steps size INC, The modified voltage conductivity algorithm.*

1. INTRODUCTION

To solve photovoltaic battery performance problems, a method is needed to get the highest power is shown by the photovoltaic system. Today, with the rapid development of power electronics and materials science, engineers have access to modern, compact power electronic systems that meet the needs of high-performance power converters. Thanks to the introduction of power electronics systems, the efficiency of photovoltaic PV cells is significantly increased, but the disadvantage of these systems is that they consume an additional amount of power. But because the cost of a photovoltaic battery system is still very high and the efficiency is still low, it cannot compete well in the electricity market and become the main source of energy.

The steady development of photovoltaic cell manufacturing techniques will make the use of this technology more widely available in practice. The application of MPPT algorithms aimed to further increase the efficiency of modules in photovoltaic cells. In this paper, an mINC algorithm based on the traditional INC algorithm with the optimal step-change voltage has shown a good result in detecting the maximum power point with strong changes in environmental conditions. school. The simulation results have shown that the mINC algorithm is more efficient than the previous old algorithms.

2. MATERIALS AND METHODS

2.1. Photovoltaic battery model

For convenience in calculation and design, an equivalent circuit is given to replace the photovoltaic battery.

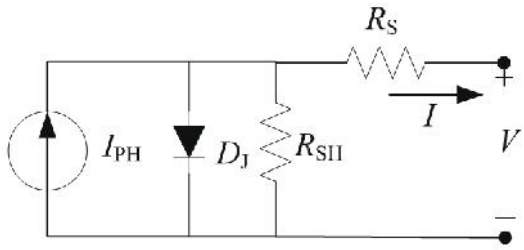

Figure 1. Equivalent photovoltaic battery circuit.

The circuit comprises output current I, output voltage V, diode (D_J), leakage current resistor R_{SH}, and series resistor R_S

A mathematical equation shown in formula 2.1 shows, to prove the relationship between the output voltage and current output of the photovoltaic cell and the voltage. It is shown in figure 1 and the equivalence between current and voltage.

$$I = I_{PH} - I_S\left[e^{\frac{q}{kT_c A}(V+I_R)} - 1\right] - \frac{V+I_R}{R_{sh}} \quad (2.1)$$

In there:

I_{PH}: Photoelectric current (A)
V & I: Cell output voltage and current (V & A)
I_s: Current reversal index of photovoltaic cell (A)
q: Charge of electrons, q = 1,6 x 10^{-19}(C)
k: Constant Boltzmann, k =1,38 x 10^{-23}(J/K)

T_C: Absolute temperature of photovoltaic cell (0^C)
A: The ideal coefficient depends on the battery technology, for example, Technology S_i-mono A=1.2, Si-Poly A = 1.3…
R_s: Resistors connected in series (Ω)
R_{sh}: Resistors connected in parallel (Ω)

Amount of batteries connected in the chain and parallel is determined by the characteristic equation shown in the PV module's characteristic equation 2.2. The experimental findings show that the resistance in series has a greater influence on current variation than parallel resistance [2].

$$I = N_p I_{PH} - N_p I_s \left[e^{q\left[\frac{\frac{V}{N_S}+I\frac{R_S}{N_p}}{kT_cA}\right]} - 1 \right] - \frac{V\frac{N_p}{N_S}+I+R_s}{R_{sh}} \quad (2.2)$$

There is
N_s: The quantity of series-connected cells.
N_p: Order to be connected in parallel.

2. Model of the grid-connected photovoltaic battery.

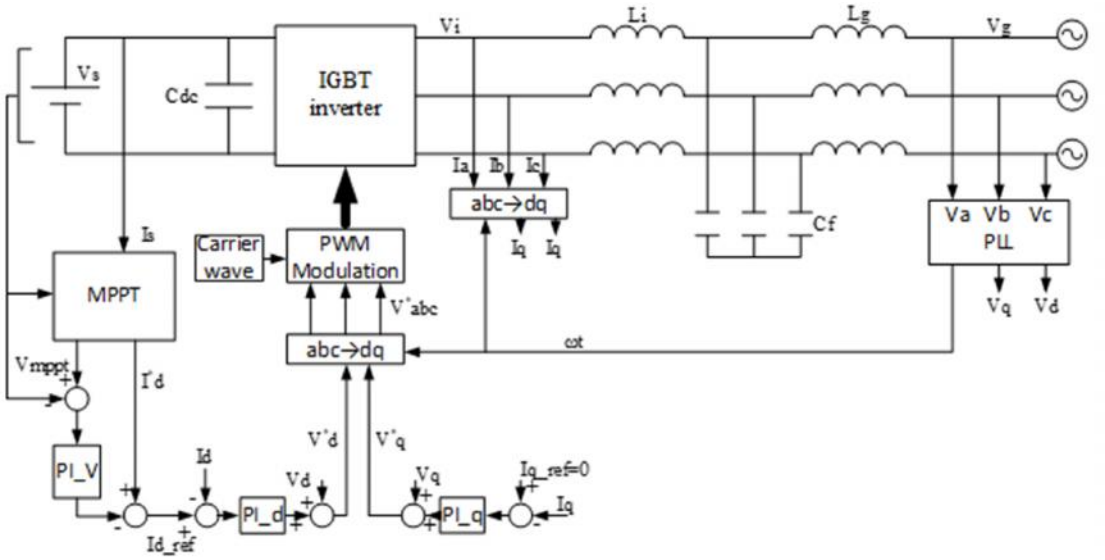

Figure 2. Grid diagram of photovoltaic battery.

The principle of operation shown in figure 2 is as follows: A conventional 6-step PWM inverter with 6 pulses is generated by comparing the high frequency carrier with the control wave. The control wave is calculated by converting the modulating signal to the control wave. control V*d and V*q into V*abc signals through the converter d_q → abc, combined with the phase angle obtained from the main voltage (via the PLL unit) to synchronize with the grid. In which, V*d and V*q are generated by adding two main voltage signals V_d and V_q with the

error of the control current (I_{d_ref} - I_d) and (I_{q_ref} - I_q) (through the corrector error P_{I_d} and P_{I_q}). With I_{q_ref} equal to 0, we have a reactive power Q pumped to the grid of 0. On the other hand, the quantity I_{d_ref} is calculated by taking the difference of the current I*d (calculated from the MPPT block) with the error of the reference voltage projection (V_{mpp} – V_s).
Models of photovoltaic cells, MPPT sets, and inverters are modeled and demonstrated using simulation software Matlab Simulink as shown in figure 3.
In addition, in this photovoltaic system, there are power conversion and control blocks that support the goal of optimal control of the photovoltaic system as shown in figure 4 and figure 5.

- Photovoltaic battery system block

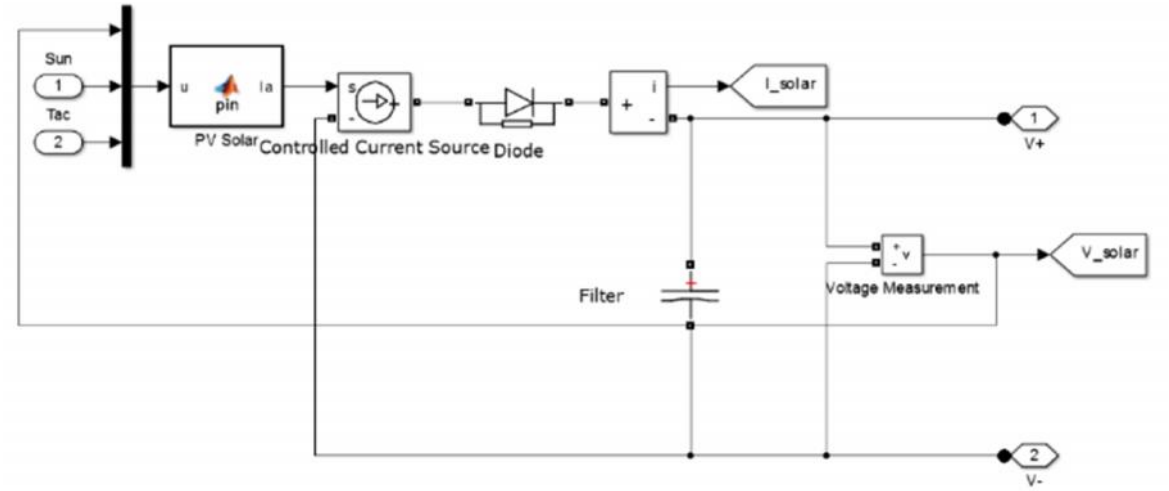

Figure 3. Simulation of the photovoltaic battery block.

- Control block

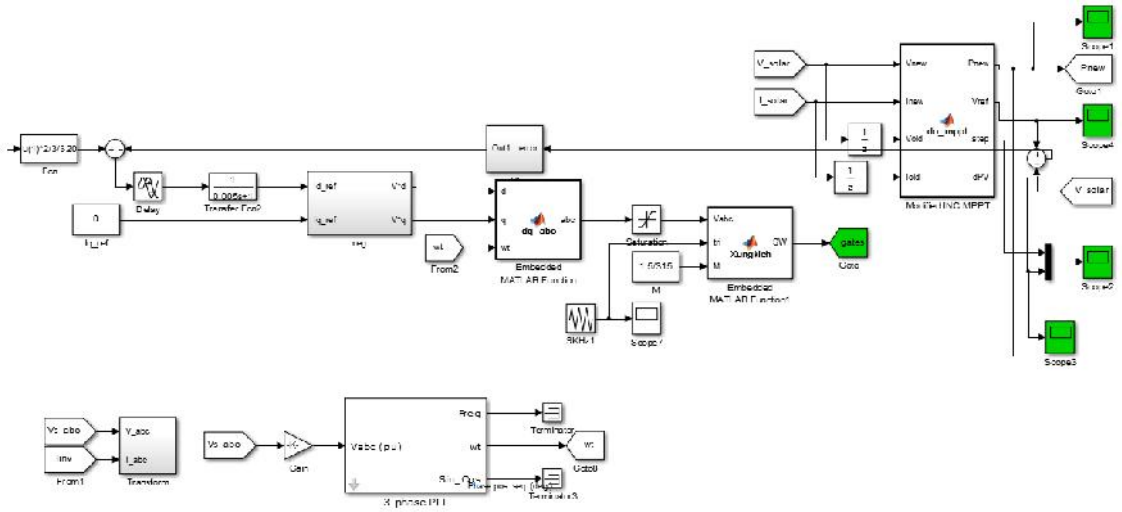

Figure 4. Simulation of control block.

- Inverter circuit block

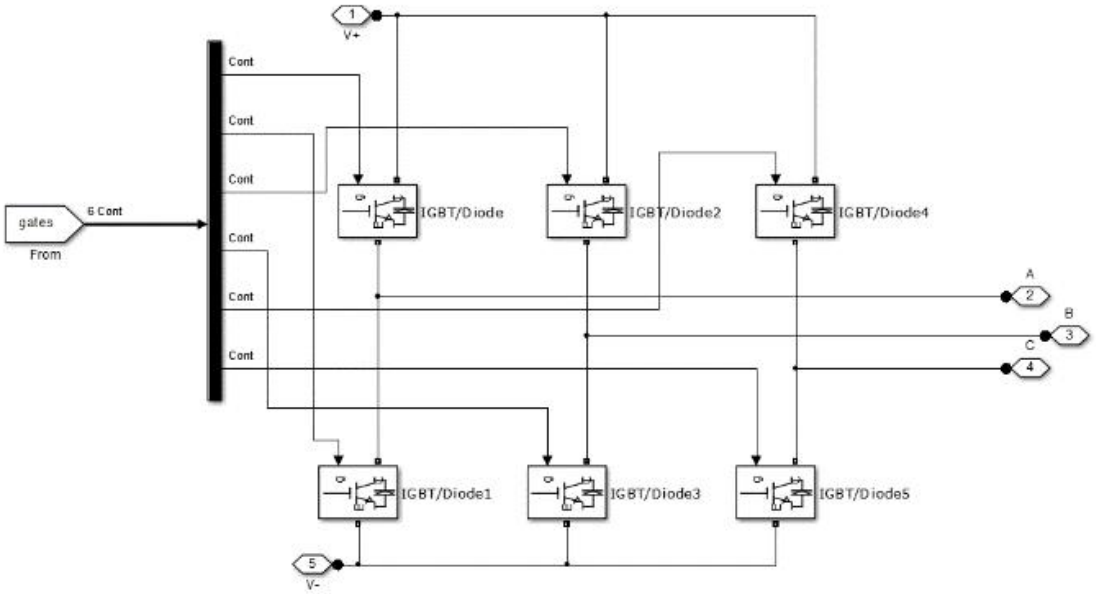

Figure 5. Simulation block of inverter circuit.

- Measurement block

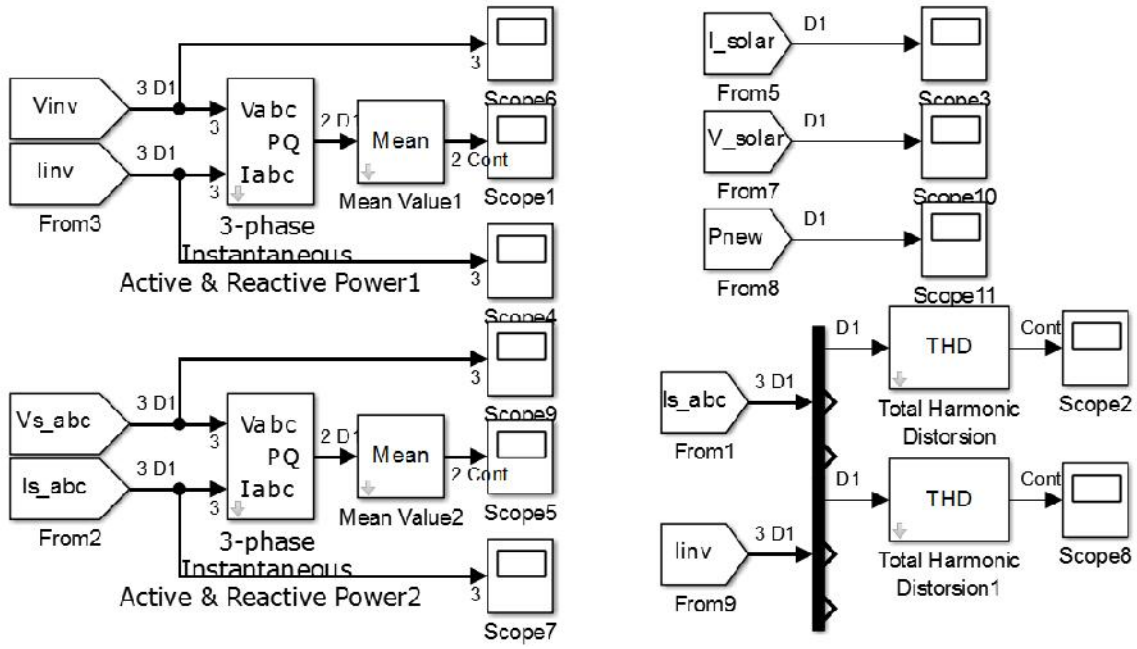

Figure 6. Measurement block simulation.

2.2. Proposed Improved INC Algorithm

At the MPP point, we can see dP/dV = 0, and when dP/dV > 0 then is the point to the left of MPP, and dP/dV < 0 then is the point to the right of MPP as shown in formula 2.3

$$\frac{dP}{dV} = \frac{(IV)}{dV} = I + V\frac{dI}{dV} \cong I + \frac{\Delta I}{\Delta V} \qquad (2.3)$$

This is how we may do it: at point MPP, dI/dV = - I/V, lies to the left of the point MPP is dI/dV > - I/V and lies to the right of the point MPP are dI/dV - I/V. Combined with the dP/dV curve as shown in Figure 7 and figure 8, we can establish an improved INC algorithm as shown in figure 9.

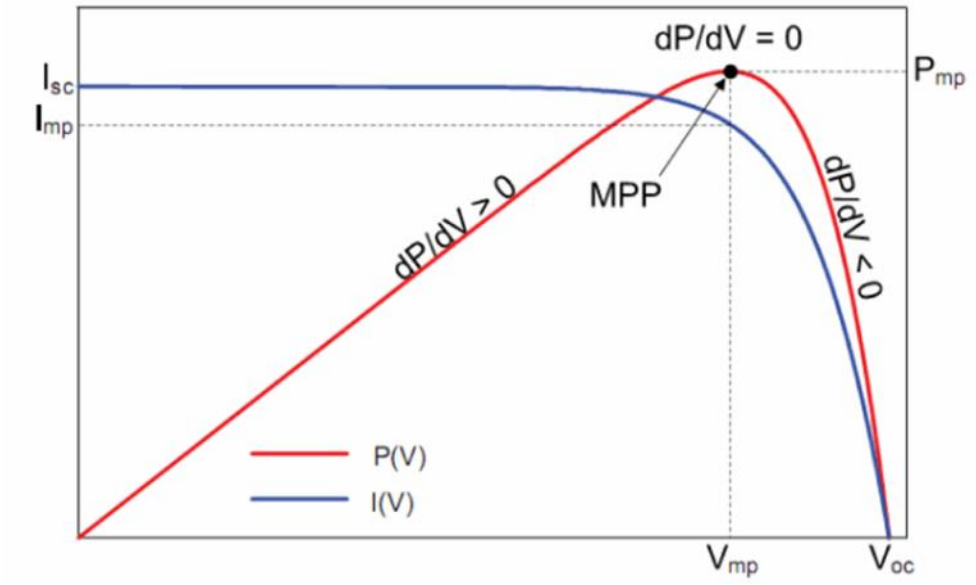

Figure 7. Slope (dP/dV) of Photovoltaic battery.

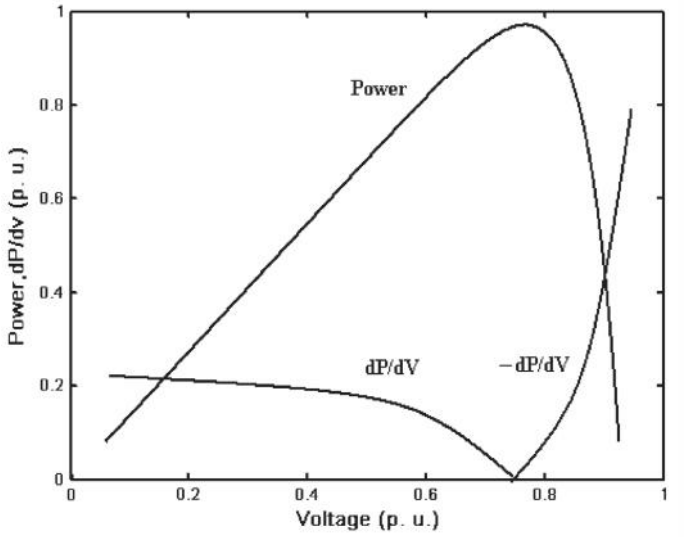

Figure 8. dP/dV. Characteristic.

The improved INC algorithm flowchart was established, Based on the algorithm flowchart, we programmed the MPPT block as follows:

```
function
[Pnew,Vref,step,dPV]=do_mppt(Vnew,Inew,Vold,Io
ld)% Intinial interation
N=1;
dV=Vnew-Vold;
dI=Inew-Iold;
Pnew=Vnew*Inew;
dP=Vnew*Inew-Vold*Iold;
step=N*abs(dP/dV);
dPV = dP/dV;
if step<=0.1
   step=0.1;
elseif step>=20
   step=20;
end
if dV=0
   if    dI==0
   Vref=Vold;
   elseif dI>0
   Vref=Vold+step;
   else
   Vref=Vold-step;
   end
else
   if    dI/dV==-Inew/Vnew
   Vref=Vold;
   elseif dI/dV>-Inew/Vnew
   Vref=Vold+step;
   else
   Vref=Vold-step;
   end
end
end
```

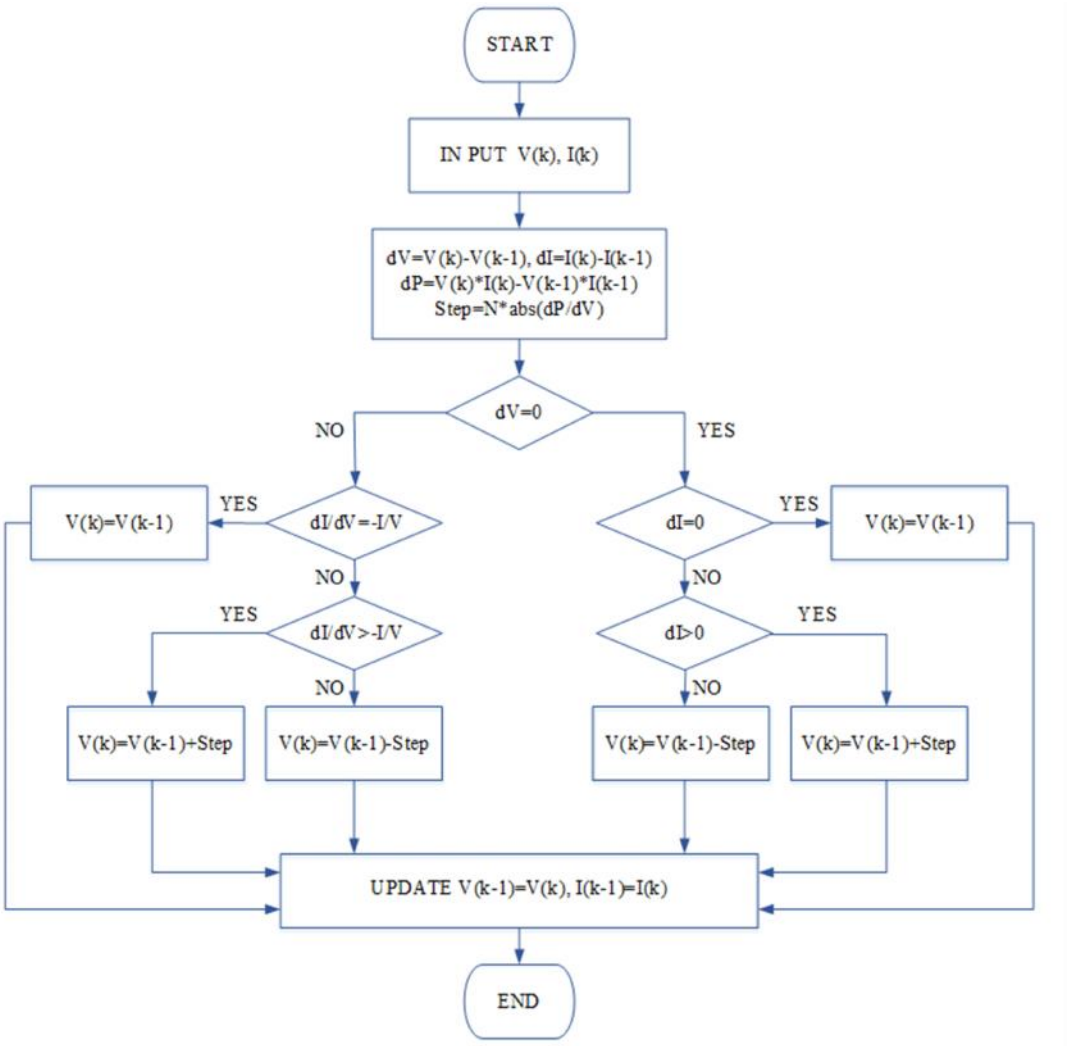

Figure 9. Improved INC Algorithm Flowchart.

3. RESULTS

The graph of solar radiation used in the simulation is described in fig 10.

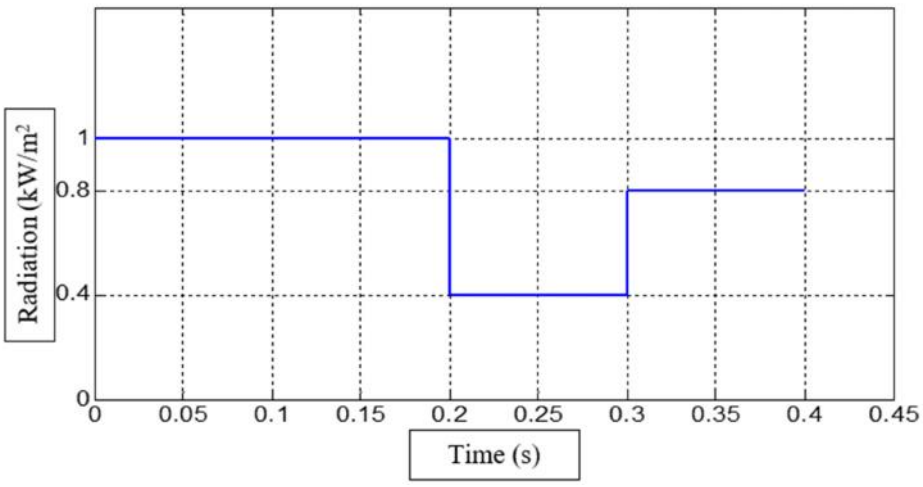

Figure 10. The graph shows the change in solar radiation.

Figure 10 shows that the change of solar irradiance with time leads to voltage increase and decrease as shown in figure 11, which shows that solar distance affects voltage change leading to efficiency rate will decrease in 0.2-0.3s.

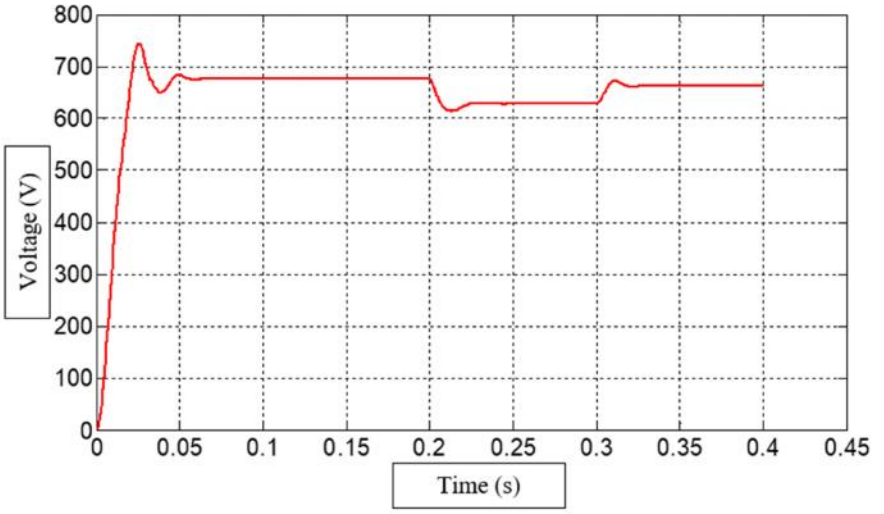

Figure 11. Graph V_{pv}.

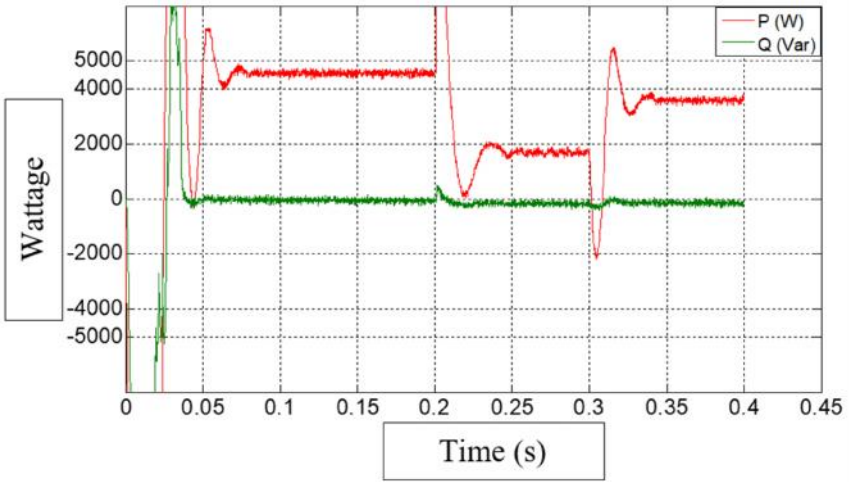

Figure 12. Graph showing the photovoltaic battery output power.

From Figures 10, figure 11, and figure 12. We see that when solar radiation changes, V_{pv} changes accordingly.

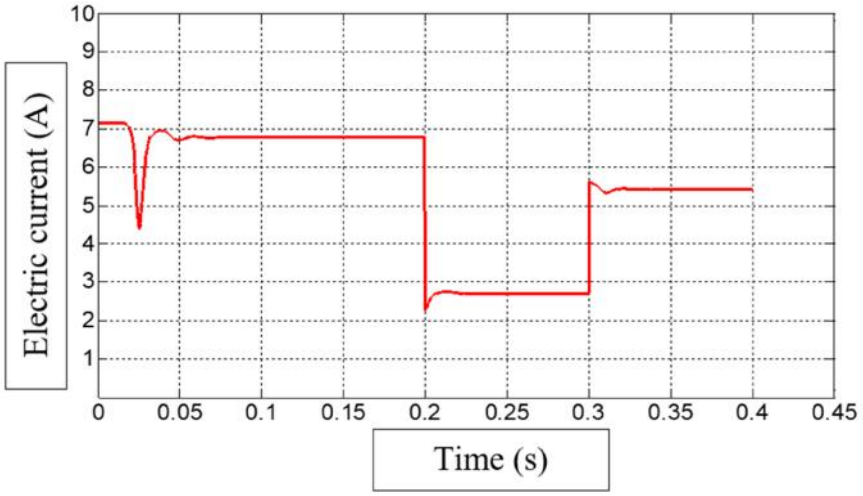

Figure 13. Graph showing the photovoltaic battery output current.

The voltage V_{pv} changes is decided by the MPPT controller and V_{pv} always ensures that $V_{pv} = V_{mpp}$, at radiation 1 (kW/m^2) the value of active power pumped into the grid reaches 4593 (W) and V_{mpp} = 676 (V), at radiation 0.4 (kW/m^2), the value of active power pumped into the grid reaches 1697 (W) and V_{mpp} = 628 (V), at radiation 0.8 (kW) /m^2) the value of active power pumped into the grid reached 3598 (W) and V_{mpp} = 663 (V). The response of the system is relatively fast within 2 cycles at the time the radiation changes (t = 2s and t = 3s) as shown in figure (11~14).

From the graph of the output current of the photovoltaic battery as shown in figure 14. We have the corresponding pump current to the grid through the inverter.

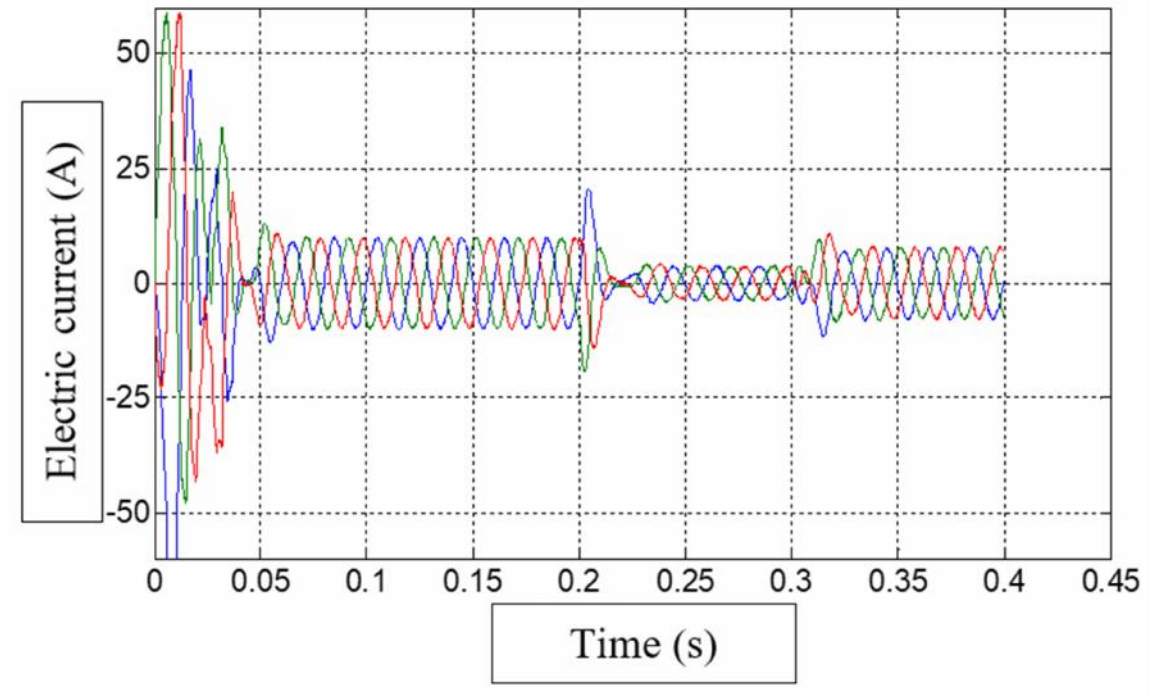

Figure 14. Graph of current pumped into the grid through the inverter.

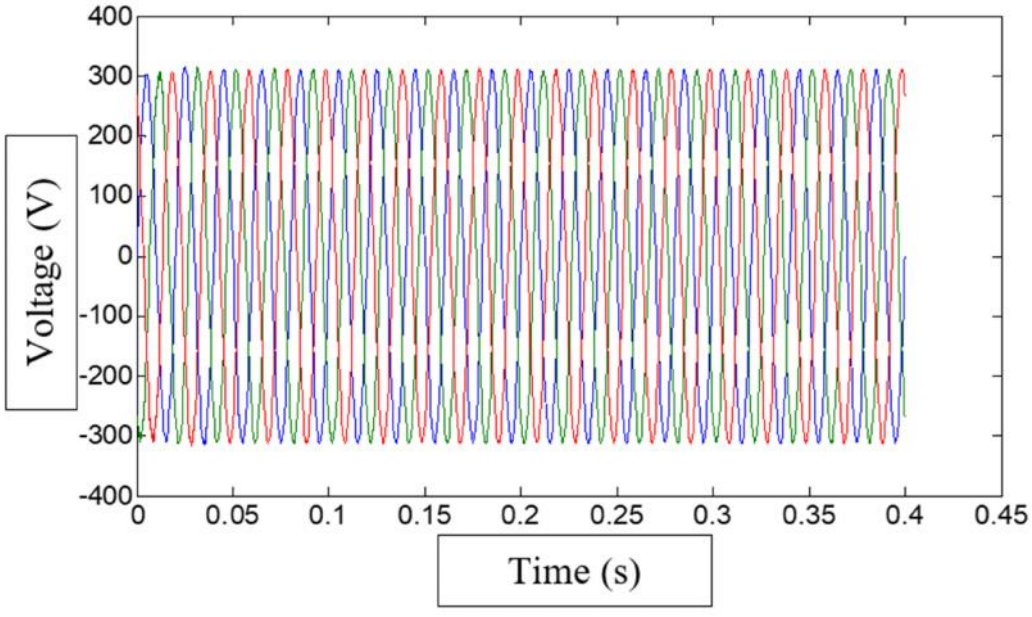

Figure 15. Grid voltage graph.

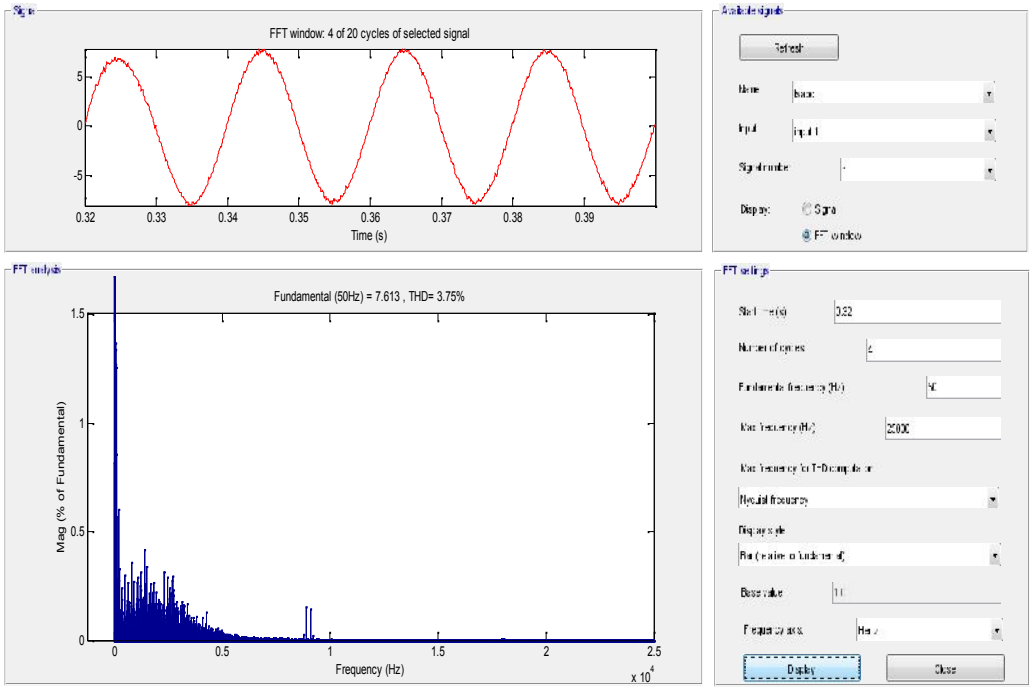

Figure 16. Harmonic parameters of current pumped into the grid.

From Figures 16 and figure 17. We can see that with the mINC algorithm, the current injected into the grid has low harmonic distortion (THD = 3.75%). Low grid voltage harmonic distortion (THD = 0.32%). According to the grid standard harmonic distortion should be less than 5 %.

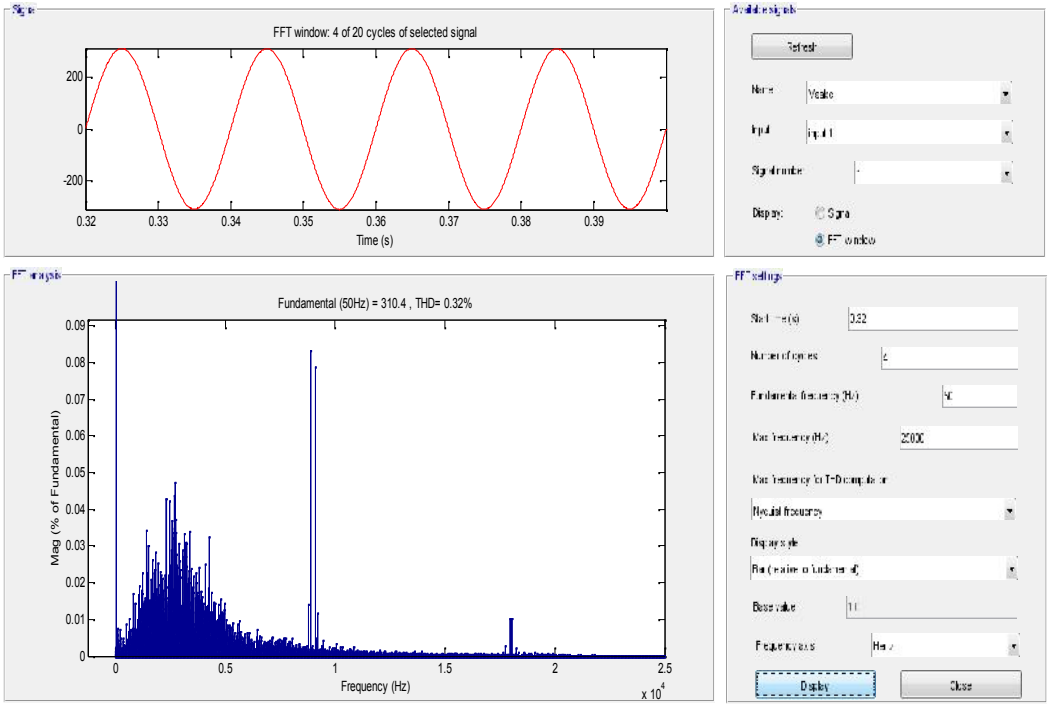

Figure 17. Grid voltage harmonic parameters.

4. CONCLUSION

Photovoltaic battery system combining MPPT controller with advanced INC algorithm shows good simulation results, fast response time, low harmonic distortion. In addition, the transient time of the system when there is a change in the intensity of solar radiation from the outside

environment does not exceed 2 cycles of distribution grid voltage, showing the ability to respond very quickly to the change. Constant solar radiation intensity of the external environment.
An inverter with a power factor of approximately 1 pumped into the grid can be considered as a simulation system that only pumps the active power component and does not pump the reactive power component to the distribution grid.

REFERENCES

Farhani, S., & Bacha, F. (2021). High efficiency power electronic converter for fuel cell system application. *Ain Shams Engineering Journal*, *12*(3), 2655-2664.

Wang, H., Tao, T., Xu, J., Shi, H., Mei, X., & Gou, P. (2022). Thermal performance of a liquid-immersed battery thermal management system for lithium-ion pouch batteries. *Journal of Energy Storage*, *46*, 103835.

Hoang, A. Q., Le, C. H., & Quang, T. C. T. (2014). Nghiên cứu lý thuyết và thực nghiệm mô hình máy lạnh hấp phụ mặt trời sử dụng Zeolite-Nước. *Journal of Technical Education Science*, (27), 23-29.

Xu, Z., Xu, J., Guo, Z., Wang, H., Sun, Z., & Mei, X. (2022). Design and optimization of a novel microchannel battery thermal management system based on digital twin. *Energies*, *15*(4), 1421.

Aldaoudeyeh, A. M. I. (2018). Development of a generalised PV model in MATLAB/Simulink using datasheet values. *The Journal of Engineering*, *2018*(5), 257-263.

Boukenoui, R., Bradai, R., Mellit, A., Ghanes, M., & Salhi, H. (2015, November). Comparative analysis of P&O, modified hill climbing-FLC, and adaptive P&O-FLC MPPTs for microgrid standalone PV system. In *2015 international conference on renewable energy research and applications (ICRERA)* (pp. 1095-1099). IEEE.

Rokonuzzaman, M., Shakeri, M., Hamid, F. A., Mishu, M. K., Pasupuleti, J., Rahman, K. S., ... & Amin, N. (2020). Iot-enabled high efficiency smart solar charge controller with maximum power point tracking—Design, hardware implementation and performance testing. *Electronics*, *9*(8), 1267.

Tsai, H. L., Tu, C. S., & Su, Y. J. (2008, October). Development of generalized photovoltaic model using MATLAB/SIMULINK. In *Proceedings of the world congress on Engineering and computer science* (Vol. 2008, pp. 1-6).

Yurchenko, D., Machado, L. Q., Wang, J., Bowen, C., Sharkh, S., Moshrefi-Torbati, M., & Val, D. V. (2022). Global optimisation approach for designing high-efficiency piezoelectric beam-based energy harvesting devices. *Nano Energy*, *93*, 106684.

Shaikh, M. N., Zafar, Q., & Papadakis, A. (2020). Development of a Comprehensive Matlab/Simulink Based Model for High-Efficiency 2nd Generation Photovoltaic (PV) Modules. *Current Nanoscience*, *16*(4), 568-577.

Villalva, M. G., Gazoli, J. R., & Ruppert Filho, E. (2009). Comprehensive approach to modeling and simulation of photovoltaic arrays. *IEEE Transactions on power electronics*, *24*(5), 1198-1208.

Liu, F., Zha, X., Zhou, Y., & Duan, S. (2009, May). Design and research on parameter of LCL filter in three-phase grid-connected inverter. In *2009 IEEE 6th International Power Electronics and Motion Control Conference* (pp. 2174-2177). IEEE.

Liu, F., Duan, S., Liu, F., Liu, B., & Kang, Y. (2008). A variable step size INC MPPT method for PV systems. *IEEE Transactions on industrial electronics*, *55*(7), 2622-2628.

Tran, T. Q., & Truong, A. V. (2012). MPPT VOLTAGE REGULATING IN THREE-PHASE GRID-CONNECTED PHOTOVOLTAIC SYSTEM. *Science and Technology Development Journal*, *15*(2), 50-61.

Jiang, L. (2012). *Resistance Control MPPT for Smart Converter PV System* (Doctoral dissertation, Virginia Tech).

Jiang, J. A., Huang, T. L., Hsiao, Y. T., & Chen, C. H. (2005). Maximum power tracking for photovoltaic power systems. *Journal of Applied Science and Engineering*, *8*(2), 147-153.

Alsadi, S., & Alsayid, B. (2012). Maximum power point tracking simulation for photovoltaic systems using perturb and observe algorithm.